Sensitizer molecular structure-device efficiency relationship in dye sensitized solar cells

John N. Clifford,* Eugenia Martínez-Ferrero, Aurélien Viterisi and
Emilio Palomares*

In the Dye Sensitized Solar Cell (DSSC) the dye sensitizer carries out the light harvesting function and is therefore crucial in determining overall cell efficiency. In addition, the dye sensitizer can influence many of the key electron transfer processes occurring at the TiO_2/dye/electrolyte interface which also determine efficiency. Dye structure can influence and drive forward electron injection into the conduction band of the TiO_2. Conversely, dye structure can help retard loss electron transfer processes such as charge recombination of injected electrons in the TiO_2 with dye cations and also recombination of these electrons with the electrolyte. Therefore tuning dye sensitizer light absorbing properties and control of the aforementioned electron transfer processes through structural design of the dye sensitizer is an important avenue through which optimization of DSSC efficiency should be pursued. In this *critical review* the latest work focusing on the design of dyes for efficient DSSCs is revised (111 references).

1. Introduction

Modern society is heavily dependent upon energy resources and their continued supply is crucial towards long term global economic and political stability. The fact that these resources are still largely based on non-renewable fossil fuels such as oil and gas and growing public concern over the environmental damage that the use of such materials may be causing has encouraged the development and exploitation of renewable forms of energy. The abundance of solar energy which bathes the earths surface in 120 000 terawatts of energy makes it extremely attractive for harnessing as a renewable energy

ICREA and Institute of Chemical Research of Catalonia, Av. Països Catalans 16, 43007 Tarragona, Spain. E-mail: epalomares@iciq.es, jnclifford@iciq.es; Fax: +34 977 920 224; Tel: +34 977 920 200

From Left to Right: John N. Clifford, Eugenia Martínez-Ferrero, Aurélien Viterisi, Emilio Palomares

Dr John N. Clifford did his PhD at Imperial College, London (UK) under the supervision of Prof. James R. Durrant working on charge transfer reactions in Dye Sensitized Solar Cells. After several post doctoral positions in Italy (Dr Nicola Armaroli, ISOF, CNR, Bologna) and Belgium (Prof. Johan Hofkens, KU Leuven) he joined the group of Prof. Palomares at ICIQ as a Juan de la Cierva Fellow. His current research interests include the control of the charge transfer reactions in "molecular dye cocktails" on mesoporous TiO_2 to achieve efficient panchromatic response in DSSCs.

Dr Eugenia Martínez-Ferrero obtained her PhD at the University of Valencia (Spain) under the supervision of Prof. Eugenio Coronado working on molecular materials with optical, electrical and magnetic properties. After a postdoctoral stay in France in the group of Prof. Clement Sánchez (UPMC, Paris) she joined the group of Prof. Palomares at ICIQ as a Juan de la Cierva Fellow.

Her work at ICIQ has focused on optimizing the properties of several semiconductor metal oxides to enhance DSSC performance as well as leading the work on hybrid light emitting devices (HYLEDs) in the group.

Dr Aurélien Viterisi did his PhD at the University of Edinburgh (UK) under the supervision of Prof. David A. Leigh working on synthetic organic and supramolecular chemistry. Aurélien joined the group of Prof. Palomares as a post doctoral fellow under the FP7-EU project ROBUST and his work is focused on the synthesis of molecular sensitizers and the study of supramolecular assemblies to achieve panchromatic sensitization in DSSCs.

Dr Emilio Palomares is ICREA Professor at ICIQ. Emilio did his PhD at the Universidad Politécnica de Valencia under the supervision of Prof. Hermengildo García. He obtained a Marie Curie Post Doctoral Fellowship to work with Prof. James R. Durrant at Imperial College London on charge transfer reactions in DSSCs. He returned to Spain to work as a Ramon y Cajal fellow at the Instituto de Ciencia Molecular-Universidad de Valencia and after a year he moved as an independent researcher to ICIQ. He has been recently awarded with an ERCstg fellowship (Polydot) and holds several awards including the Young Spanish Chemist Award by the Spanish Royal Society of Chemistry.

source. Indeed, for many this is the holy grail of renewables. Single crystal silicon solar cells are currently the paradigm in solar cell technology achieving over 25% conversion efficiency in the best modules. However these cells are still too expensive for large scale production, even taking into account the high price of oil currently on the world market.

Dye Sensitized Solar Cell (DSSC) are currently the leading photovoltaic alternative to silicon based solar cell technology. They are attractive not only because of the possibility of harnessing solar energy providing a clean and abundant energy source but also because in large scale production their fabrication cost would be expected to be a fraction of that of the silicon solar cell. DSSCs consist of a porous nanocrystalline film of typically TiO_2 nanoparticles (~ 20 nm diameter) immobilized onto a conducting material which is sensitized to visible light through the adsorption of a monolayer of dye. The cell is completed by a liquid electrolyte, typically the iodine/tri-iodide red–ox couple in acetonitrile, and a platinum counter electrode.

A key difference between DSSCs and silicon solar cells is that light absorption and electron/hole transport is not performed by the same material. In DSSCs the light absorption function is fulfilled by the dye and the electron and hole transporting are fulfilled by the nanocrystalline metal oxide and electrolyte respectively. Therefore the absorption properties of the dye dictate the light-harvesting capacity of the cell. Moreover the dye will dictate the colour of the cell, which makes this technology architecturally interesting for incorporation into homes and buildings thereby performing an aesthetic as well as practical function. The properties that a dye sensitizer should have are the following:

-Anchoring groups such as carboxylates or phosphonates which are capable of covalently bonding to –OH groups on the TiO_2 surface.

-Optimum absorption overlap with that of the solar spectrum for efficient light-harvesting.

-Correct alignment of LUMO and HOMO energy levels with those of the TiO_2 conduction band and the iodide tri-iodide red–ox electrolyte ensuring efficient electron injection and dye regeneration.

-Capability of performing photocurrent generation over prolonged periods of illumination.

Fig. 1 shows the electron transfer processes occurring in a DSSC under operating conditions. Following the absorption of a photon of energy (1) the dye sensitizer injects an electron into the conduction band of the TiO_2 from the S* excited state (2). This electron percolates through the film to the back contact where it travels through an external circuit performing work (3). Oxidized dye cations S^+ are reduced by the red–ox couple (4) which is itself reduced at the platinum counter electrode (5). The possible loss mechanisms in the cell which are critical to cell performance are charge recombination of injected electrons with the oxidized dye S^+ (a) and recombination of injected electrons with the oxidized electrolyte (b), or 'dark current'.

Optimization of DSSC efficiency is being addressed in a variety of ways, for example through the design of different metal oxide materials with different nanostructures,[1] or by the development of different electrolytes including ionic
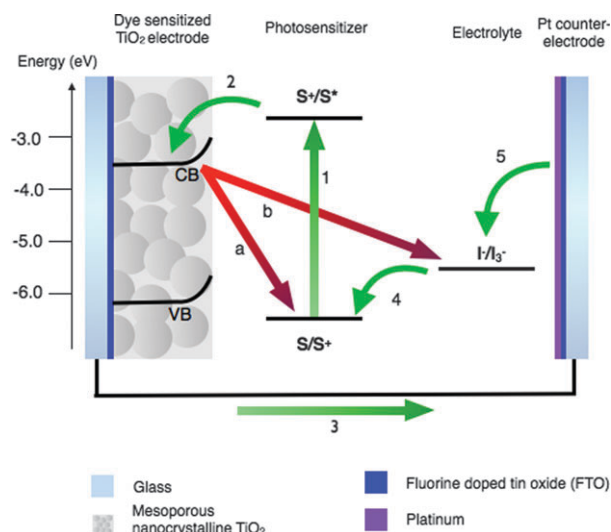

Fig. 1 Schematic representation of the electron transfer processes occurring in DSSCs.

liquids[2] and solid state hole conducting materials.[3,4] This *Critical Review*, however, will focus principally on how optimization of DSSC performance can be achieved through structural design of the dye sensitizer alone. We discuss how design can impact upon the electron transfer processes occurring at the TiO_2/dye/electrolyte interface shown in Fig. 1, namely electron injection, charge recombination and the dark current. We also discuss strategies to improve DSSC light-harvesting by the design of single sensitizers with broad absorption profiles and by sensitization with more than one dye (co-sensitization). Finally, we also highlight some examples where supramolecular principles have been utilized in the design of new sensitizers.

2. Sensitizer control of electron transfer in DSSCs

There are several excellent reviews covering the large body of experimental work on electron transfer reactions in DSSCs and the mechanisms underpinning them.[5–9] In this section these reactions are discussed, in particular how they can be tuned through molecular design of the dye sensitizer. Several studies are highlighted involving most of the commonly employed sensitizer classes used in DSSC research today.

2.1 Marcus theory applied to DSSCs

In the study of electron transfer dynamics in DSSCs, Marcus non-adiabatic electron-transfer theory[10] can be used. A quantum mechanical description of electron transfer is applied in terms of electron tunnelling from the donor to the acceptor through an insulating barrier. The penetration of the electron through the barrier will fall off exponentially with distance r:

$$H_{AB}{}^2 = H_0{}^2 e^{-\beta r} \quad (1)$$

where $H_{AB}{}^2$ represents the electronic coupling of the donor and acceptor and β is the resistance of the barrier to the penetration of the electron wavefunction. β is a property of the medium comprising the insulating barrier region and related to the

height of this barrier. The rate of electron transfer (k_{et}) incorporating this tunnelling description is given by Fermi's Golden Rule:

$$k_{et} = H_{AB}{}^2 FC = \frac{e^{-\beta r}}{\sqrt{(4\pi\lambda k_\mathrm{B}T)}} \exp\left(\frac{-(\Delta G^0 + \lambda)^2}{4\lambda k_\mathrm{B}T}\right) \quad (2)$$

where FC represents the Frank–Condon factor which expresses the energetics of the donor and acceptor states. Though Marcus theory was developed to explain the rates of electron transfer in non-covalently bound donor–acceptor complexes in solution, it can also be applied to interfacial electron transfer involving molecular species immobilized on bulk semiconductor/metallic surfaces.[11,12] In this case it is necessary to integrate eqn (2) over all possible donor or acceptor states on the electrode surface.

In eqn (2) there are four possible parameters which can vary (fixing T equal to room temperature) that can affect electron transfer: β, λ, r and ΔG^0. The first two, the barrier height β and the reorganizational energy λ, are not easily controllable parameters. β is a function of the intervening media between the donor and acceptor and λ is largely dependent upon the polarity of the surrounding solvent environment. The second two parameters however, r and ΔG^0, the donor–acceptor distance and the difference in their energies are much more amenable to change through modifications to dye structure. The effect of these parameters on several of the electron transfer reactions in DSSCs is discussed in the following sections.

2.2 Electron injection

Many early studies dedicated to understanding electron transfer in DSSCs were focused on electron injection from the photo-excited dye sensitizer into the conduction band of the nanocrystalline metal oxide. These and later studies showed ultrafast electron injection kinetics occurring on subpicosecond time scales for a variety of sensitizer dyes several orders of magnitude faster than emission decay lifetimes resulting in extremely efficient charge separation.[13–20] Moreover, the kinetics of electron injection were found to be non-exponential in nature, which is attributed to a variety of factors including surface heterogeneity of the metal oxide, different sensitizer anchoring modes and injection from a variety of different excited states (i.e. singlet, triplet etc.). Ultrafast injection is often explained in terms of the strong electronic overlap of the LUMO orbitals of the dye and the acceptor states on the metal oxide electrode. In **N3/N719** for example, the HOMO is located mainly on the ruthenium metal and –NCS ligands whereas the LUMO is located on the π^* orbitals of the bipyridyl ligands. As these bipyridyl ligands are directly anchored to the electrode surface through the –COOH anchoring groups, photo-excitation results in a shift in excited state electronic density towards the metal oxide surface. The most efficient organic sensitizers also display this directional shift in excited state electron density towards the anchoring ligands and therefore good electronic overlap with the acceptor states of the metal oxide surface. Fig. 2 shows the chemical structure, optimized molecular structure and frontier molecular orbitals for the organic dye **JK1**.[21] The
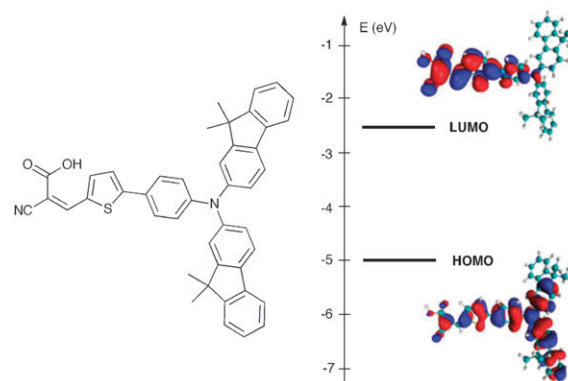

Fig. 2 Chemical structure and HOMO/LUMO frontier molecular orbitals of organic dye **JK1**.

HOMO is delocalized over the bis-dimethyl-fluorene aniline ligand whereas the LUMO is situated on the opposite end of the molecule with significant electron density over the –COOH anchoring unit indicating that photo-excitation of this sensitizer will result in migration of electron density towards the electrode surface.

While Ru(II) bipyridyl and organic sensitizers of general type donor–(π-bridge)–acceptor (see section 3) can effectively channel excited state energy towards the TiO$_2$ surface, such directionality in the excited state for symmetrical porphyrin and phthalocyanine sensitizers is problematic. This is because the HOMO and LUMO of these highly symmetrical sensitizers (e.g. **ZnTPP**[22], Fig. 3) are effectively delocalized over the entire conjugated π-ring system. Directionality of excited state energy and improved electronic coupling between these sensitizers and TiO$_2$ can be achieved with unsymmetrical structures such as **DPA–ZnP–COOH**[23] (Fig. 3) which when utilized in DSSCs shows an excellent efficiency of 6% with improved J_{sc}. In fact the structure of **DPA–ZnP–COOH** rather reminds one of the donor–(π-bridge)–acceptor structural motif very common for organic sensitizers today.[24] In the case of **DPA–ZnP–COOH** one can consider the π-bridge to be in fact the porphyrin ring itself. Unsymmetrical phthalocyanine sensitizers have also shown higher efficiencies and J_{sc} in DSSCs than their symmetrical counterparts.[25]

The dependence of the rate of electron injection upon the distance and free energy parameters in agreement with Marcus non-adiabatic electron-transfer theory as discussed in section 2.1 has been investigated. Variation of the distance r between the dye excited state and the metal oxide surface was
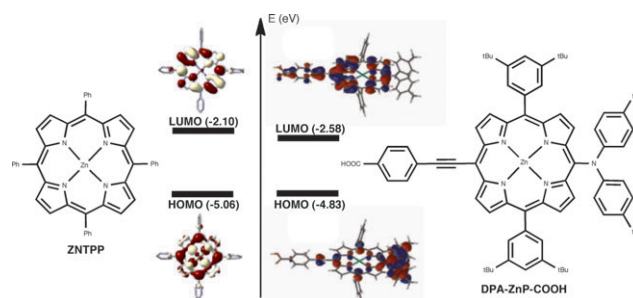

Fig. 3 Chemical structure and HOMO/LUMO frontier molecular orbitals of **ZnTPP** and **DPA–ZnP–COOH**. Adapted from ref. 22 and 23.

achieved through the use of spacer groups. Lian and co-workers[26,27] varied this distance by employing –CH$_2$– spacers for a series of three sensitizers **Re(bpy(CH$_2$)$_{2n}$(COOH)$_2$)CO$_3$Cl** (n = 1–3) on nanocrystalline SnO$_2$ films. **Re(bpy(CH$_2$)$_2$(COOH)$_2$)CO$_3$Cl** (*i.e.* where n = 1) showed ultrafast (<100 fs) electron injection whereas slower injection times were found with the other two sensitizers (19 and 240 ps where n = 2 and 3 respectively) showing a clear dependency of electron injection upon distance. (Interestingly, this study and others[28–32] demonstrated that intimate coupling of the LUMO of the sensitizer and metal oxide surface is not a necessary prerequisite for electron injection to occur). Probing the effect of free energy ΔG^0 upon electron injection can be done by either modulating the Fermi level of the metal oxide or by changing the red–ox potential of the dye sensitizer anchored to it. The former was done by Durrant and co-workers[33] by incorporating an **N3** sensitized TiO$_2$ electrode into a three electrode cell and applying a bias and the latter as part of the study discussed above by Lian and co-workers[26] by using a series of different **Ru(dcbpy)$_2$X$_2$** dyes where (X$_2$ = 2SCN$^-$, 2CN$^-$ and dcbpy) with different ground and excited state red–ox potentials immobilized onto SnO$_2$. In both studies the rates of electron injection were found to be dependent upon free energy differences.

Large π-conjugated sensitizers such as porphyrins and phthalocyanines and organic sensitizers such as coumarines and perylenes have a marked tendency towards aggregation in solution and on the surface of TiO$_2$ and this is one of the reasons why they have generally shown lower efficiencies in DSSCs. Aggregation can quench dye excited states resulting in lower injection yields.[34–36] One way to avoid aggregation is to sensitize in solutions containing coadsorbates such as chenodeoxycholic acid[37,38] which can help break up dye aggregates on the TiO$_2$ surface leading to improved cell efficiencies. However, even in the presence of these adsorbates aggregation can still be a problem. In this case the need to employ sensitizers whose structures have been specifically designed to impede aggregation is unavoidable. Employing peripheral units bearing bulky side groups such as *tert*-butyl can effectively minimize aggregation resulting in higher J_{sc} (and therefore more efficient electron injection) and an overall improvement in cell efficiencies.[25] Another strategy to reduce aggregation in phthalocyanines is to anchor them in a parallel fashion to the TiO$_2$ surface using ligands which can axially co-ordinate the central metal atom. In this case it is necessary to use 5 and 6 coordinate metals such as Ti and Ru.[31,32]

2.3 Charge recombination of injected electrons with *dye*$^+$

In stark contrast to the ultrafast nature of electron injection, charge recombination manifests itself as a rather slow reaction occurring on micro- to millisecond timescales and of a highly dispersive nature.[18,39] The reason for such slow recombination has generally been ascribed to slow electron transport in the TiO$_2$ film due to trapping/detrapping[40,41] with lifetimes showing a strong dependence upon electron occupancy within the metal oxide.[39] The effect of sensitizer molecular structure on recombination has been investigated in many studies. Addition of secondary electron-donating groups to
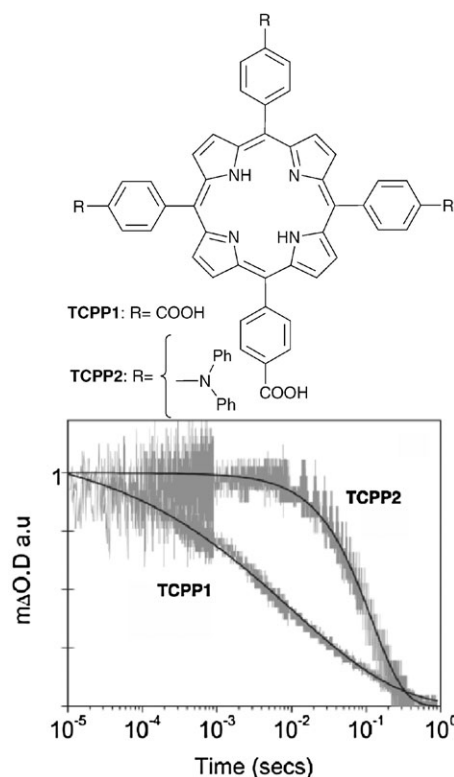

Fig. 4 Chemical structure (top) of porphyrins **TCPP1** and **TCPP2** and recombination kinetics (bottom) of these dyes on nanocrystalline TiO$_2$ film. Adapted from ref. 42.

sensitizer structure, increasing the distance between the dye cation centre and the TiO$_2$ surface has been shown to effect the rate of charge recombination for a number of sensitizers.[42–44] For example, Durrant[42] and co-workers modified the porphyrin **TCPP1** by substituting three of the –COOH groups for triphenylamines and observed a retardation in recombination dynamics by more than one order of magnitude (Fig. 4). Moreover, the shape of the dynamics change from stretched exponential to monoexponential indicating that recombination has moved from a TiO$_2$ transport limited to interfacial limited regime.

The effect of free energy ΔG^0 and distance r parameters upon charge recombination was also investigated by Durrant[45] and co-workers. Charge recombination was measured for TiO$_2$ films sensitized with a variety of sensitizers including Ru(II) polypyridyls, phthalocyanines and porphyrins. As these dyes have different ground state oxidation potentials (by up to 500 mV) free energy ΔG^0 of recombination was varied. The different dye structures allow the distance r parameter to be modulated by several nanometres (estimated from HOMO/ LUMO calculations). Recombination lifetimes show a clear dependence upon distance r with no correlation between lifetime and free energy ΔG^0 observed. This study underlines the importance of dye structure for achieving effective charge separation in DSSCs: just as for electron injection where one should consider the LUMO of the dye sensitizer to achieve strong electronic coupling with TiO$_2$, the cation centre on the dye sensitizer must also be considered to minimize charge recombination.

2.4 Charge recombination of injected electrons with *electrolyte*$^+$

As discussed in the previous section, charge recombination for optimized DSSC devices is generally quite slow. In fact it is sufficiently slow to allow for efficient regeneration of *dye*$^+$ by the iodide/tri-iodide liquid electrolyte. Of principle concern therefore is the recombination reaction between injected electrons in the TiO$_2$ electrode and the oxidised electrolyte, or the "dark current". V_{oc} of optimized DSSCs could be as high as 0.92 V, as noted recently by Snaith,[46] however optimized devices typically only achieve values of 700–800 mV. One key reason for this disparity is caused by the leakage of injected electrons into the electrolyte and is key to achieving higher efficiencies for these devices.

The molecular structure of the dye sensitizer can play a key role in minimizing the dark current. It can act as a barrier impeding this reaction by forming a compact monolayer on the TiO$_2$ surface.[47] Furthermore, amphiphilic dyes including **Z907**[48–50] which contain long alkyl chains can block the approach of the charged oxidized electrolyte towards the TiO$_2$ surface. DSSCs made from **Z907** show improved V_{oc} indicating dark current suppression. Alkyl chains have also been incorporated into the structures of other dye sensitizers to improve V_{oc}.[51–56]

A curious phenomena is that DSSCs made from highly conjugated dye sensitizers such as porphyrins, phthalocyanines and organic sensitizers generally show poorer V_{oc} indicating that dark current is a significant problem limiting the efficiency of these devices. Measurement of electron lifetimes in functioning DSSCs at open circuit can be used as a means of rationalizing V_{oc} for different devices.[57] Mozer and Mori[58] compared electron lifetimes of DSSCs made with **N719** and Zn porphyrin sensitizers and the shorter electron lifetimes for the latter were used to explain the roughly 150 mV lower V_{oc} for these devices. O'Regan and co-workers[59] compared electron lifetimes of DSSCs of **N719** and Ru phthalocyanine and the electron lifetimes were also shown to be much shorter for the devices based on the highly conjugated Ru phthalocyanine. Mori and co-workers[60] compared electron lifetimes in devices for a series of eight different organic sensitizers including donor–(π-bridge)–acceptor type dyes and indoline dyes compared to devices made with Ru(II) polypyridyl dyes **N719** and **N749** (black dye). In all cases the electron lifetimes were much shorter for the organic dye based devices than either the **N719** or **N749** based devices.

The correlation between lower V_{oc} and fast electron lifetimes in functioning devices appears clear, however the reasons for this and the role dye structure plays in determining it is still under discussion. Even seemingly innocuous changes to sensitizer structure can have an enormous effect on cell voltage as demonstrated in two recent studies. O'Regan[61] and co-workers measured electron lifetimes and cell efficiencies for DSSC devices made with two Ru(II) polypyridyl dyes, **TG6** and **K19** (see Fig. 5) whose structures differ by only two atoms (sulfur and oxygen). The re–dox and absorption properties of these sensitizers are essentially the same, however, devices made with **TG6** show faster electron lifetimes and inferior V_{oc}. This difference was explained by the
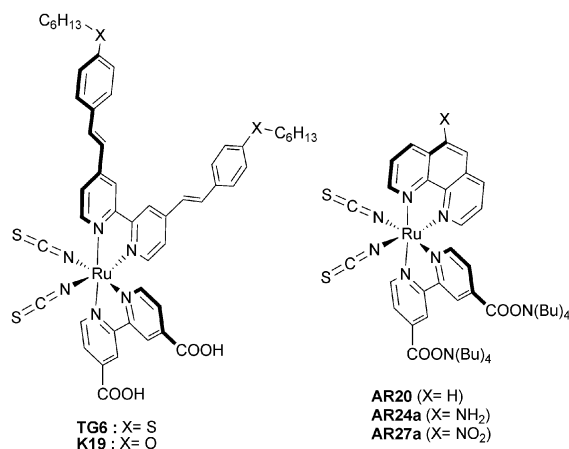

Fig. 5 Chemical structures of Ru(II) polypyridyl sensitizers **TG6**, **K19**, **AR20**, **AR24a** and **AR27a**.

difference in iodine binding of the two sensitizers with the oxygen atom of **K19** inducing a lower binding constant than that of the sulfur atom of **TG6**. In another study by Reynal *et al.*[62] the presence of electron-donating –NH$_2$ in **AR24a** and electron-withdrawing –NO$_2$ in **AR27a** (Fig. 5) has a detrimental effect upon electron lifetime, cell voltage and ultimately cell efficiency for DSSC devices made with these dyes in comparison to devices made with the reference dye **AR20**.

3. Sensitizer state-of-the-art

Since the demonstration by Grätzel and O'Regan[63] in 1991 of the first efficient DSSC of 7% based on nanocrystalline TiO$_2$, the best cell performances have continued to be recorded with Ru(II) polypyridyl dyes.[64] The 10% efficiency barrier was broken by **N3**[65] (or its di-tetrabutyl-ammonium salt equivalent **N719**)[66] and indeed this was the dye *par excellence* for many years in the field. Ru(II) polypyridyl complexes have continued to evolve, becoming ever more structurally advanced in order to address some of their drawbacks when employed in DSSCs. Such drawbacks include their limited absorbance at longer wavelengths for which **N749**,[67,68] or "black dye" (see section 4) was developed, or their long term stability for which amphiphilic dyes containing long alkyl chains such as **Z907**[49,50] (see section 2.4) were developed. Another key issue is their limited extinction coefficients (**N719** has an ε of 13 900 M^{-1} cm^{-1} at 541 nm).[66] This requires that devices are made using TiO$_2$ films over 8 μm thick to efficiently capture all of the incident light. Thicker films result in both lower V_{oc} (due to increased dark current) and lower fill factor (due to an increase in electrolyte resistance). To this end, a number of polypyridyl amphiphilic heteroleptic sensitizers such as **K19**,[69] **K77**,[70] **C101**,[71] **CYC-B1** (**Z991**)[72] and **CYC-B11**[73] have been developed for use in DSSCs (Fig. 6). These dyes which incorporate thiophenes or phenylenevinylenes into the ancillary bipyrpidyl ligands show higher ε values (24 200 M^{-1} cm^{-1} at 554 nm for **CYC-B11**), in addition to a shift in the onset of photocurrent wavelength to the red. Indeed **C101** is currently one of the best dye sensitizers used in DSSCs with efficiencies of over 11% recorded.
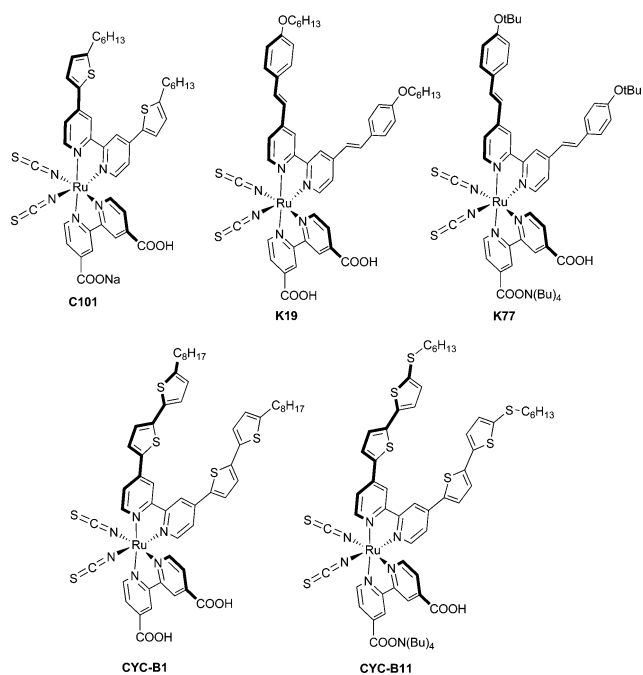

Fig. 6 Chemical structure of Ru(II) polypyridyl sensitizers **C101**, **K19**, **K77**, **CYC-B1** and **CYC-B11**.

Organic sensitizers[24] are an attractive alternative to Ru(II) polypyridyls as they do not contain any toxic or costly metal and their properties are rather easily tuned by facile structural modification. In addition, they generally have much higher extinction coefficients when compared to Ru(II) polypyridyls, often higher than $100\,000\ M^{-1}\ cm^{-1}$, making them excellent for use in solid state DSSCs utilising hole transporting materials such as P3HT[3] or OMeTAD[4] in which thinner device architectures are required. However there are a number of limitations regarding organic dyes including narrow absorption bands, aggregation, poor absorption in the red and poor stability. DSSCs utilising organic sensitizers initially showed very poor performances. However studies by Arakawa and Hara[74–77] involving coumarine dyes and Horiuchi and Uchida[78,79] using indoline dyes showed their promise so that by 2005 DSSC devices were already showing efficiencies of almost 8% with, for example, the sensitizer
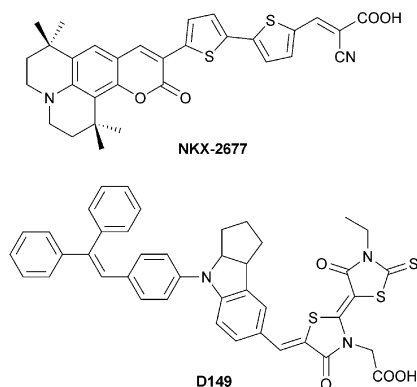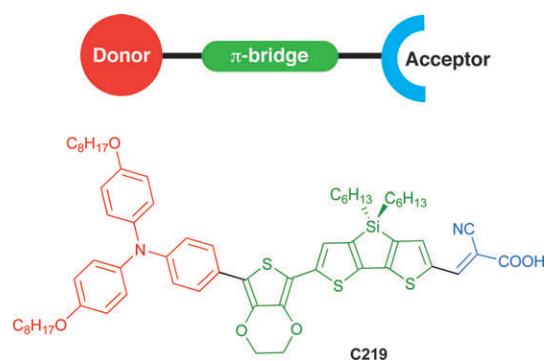

Fig. 8 Top: scheme depicting the donor-(π-bridge)-acceptor general structure. Bottom: chemical structure of **C219** organic dye.

NKX-2677 (Fig. 7) and by 2006 Ito and co-workers [80] had achieved the extremely impressive efficiency of 9% with the indoline dye **D149** (Fig. 7).

Many more recent organic sensitizers have achieved efficiencies which closely rival those of Ru(II) polypyridyls in DSSCs.[21,54,55,81–84] Indeed a recent study involving the dye **C219** (Fig. 8) showed an efficiency of over 10%.[85] These sensitizers all have the same structural motif in common, namely donor–(π-bridge)–acceptor where red–ox and absorption properties can be tuned by the judicious selection of the individual units. The most common donors used are arylamines while the acceptor is usually the cyanoacrylate group. The π-bridge often consists of one or more thiophene units. Molecular orbital calculations for these sensitizers have shown that the HOMO is located on the arylamine donor unit whereas the LUMO is centred on the cyanoacrylate anchoring group resulting in efficient electron injection into TiO$_2$. Stability tests have found these sensitizers to be extremely promising for use in DSSCs.[54,84]

Porphyrins and phthalocyanines[86] are also interesting candidates as sensitizers for DSSCs. They are highly robust, being both photo- and electrochemically stable. Moreover they are excellent light-harvesters with high extinction coefficients. Porphyrin absorption is centred mainly on the intense Soret band at 400 nm and moderate Q-bands at 600 nm. Phthalocyanines display an intense Q-band located at around
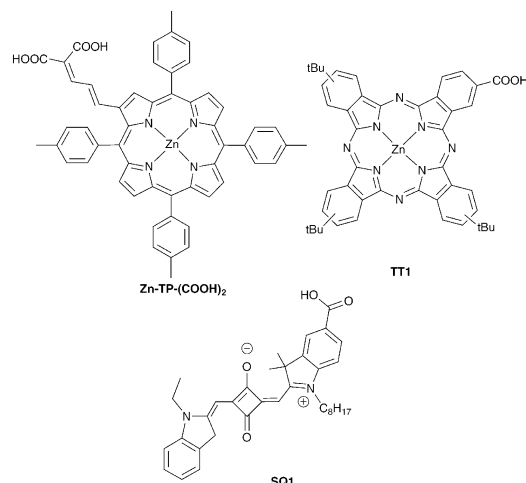

Fig. 7 Chemical structures of coumarin **NKX-2677** and indoline **D149**.

Fig. 9 Chemical structure of dyes **Zn–TP–(COOH)$_2$**, **TT1**, and **SQ1**.

700 nm due to the smaller band gap for these highly conjugated π-aromatic systems. As discussed in section 2.2, porphyrins and phthalocyanines display certain limitations for use in DSSCs such as an inherent lack of directionality in the excited state for symmetrical structures and a tendency towards aggregation. Achieving better excited state directionality can be overcome by breaking the symmetry of these large planar π-aromatic systems and designing unsymmetrical complexes such as **Zn–TP–(COOH)₂**[87] and **TT1**[25] (Fig. 9) which are currently two of the most efficient porphyrin and phthalocyanine dyes utilized in DSSCs with efficiencies of 7.1% and 3.5% respectively. In addition, substitution of **Zn–TP–(COOH)₂** at the β position of the porphyrin ring with the conjugated diethenyl linker and carboxylic acid groups results in a red shift in the Soret and Q-bands giving better absorption in the UV-visible. The staggered aryl substituents at the α positions of the porphyrin ring of **Zn–TP–(COOH)₂** and the bulky *tert*-butyl groups on **TT1** help to minimize aggregation in these complexes when bound to TiO₂.

Near-IR absorbing squarine dyes such as **SQ1**[88] (Fig. 9) are also under investigation as sensitizers for DSSCs. Similar to phthalocyanines they also show intense absorption bands but efficiencies have so far not greatly exceeded those of the phthalocyanines such as **TT1**.

4. Towards panchromatic sensitization

As already mentioned in section 1, one of the properties that an ideal dye sensitizer should possess is a broad absorption band with optimum overlap with that of the solar spectrum. The most efficient Ru(II) polypyridyl sensitizers are noticeably poor light-harvesters at longer wavelengths. For example, the incident-photon-to-current efficiency (IPCE) of **C101** ranges from 400 to 800 nm, only exceeding 80% from 480 to 660 nm.[71] The development of panchromatic single sensitizers is however rather challenging as absorption of lower energy photons towards the near-IR means the sensitizer band gap will have to be sufficiently small. Such a small band gap may compromise other properties of the dye such as, for example, ground and excited state red–ox properties which are already tuned for efficient electron injection into the TiO₂ and regeneration of the oxidized form of the sensitizer by the iodide/tri-iodide re–dox couple.

The first notable attempt to develop a panchromatic sensitizer for DSSCs was the Ru(II) polypyridyl dye **N749**,[67,68] or "black dye" (Fig. 10) containing a carboxylated terpyridyl ligand and three thiocianate groups. The three thyocianato anionic ligands stabilize the excited states by

electron donation to Ru causing the red shift of the MLCT bands by decreasing the π^* level of the 4,4′,4″-tricarboxy-2,2′ : 6′,2″-terpyridine ligand and an increase in the energy of the t_{2g} metal orbital. The resulting photovoltaic devices using **N749** exhibit impressive near-IR photoresponse with an absorption threshold of 920 nm and a plateau higher than 70% between 400 and 700 nm. However the overall efficiencies of these devices are not significantly better than cells made with **N719**. More recently a new Ru(II) polypyridyl complex with the ligand 2,6-bis-(4-carboxyquinolin-2-yl)pyridine has shown 35% IPCE at 900 nm.[89] Although overall efficiencies of devices made with this sensitizer are lower than for **N749**, to date this is the highest IPCE value reported in the near IR region for a Ru(II) polypyridyl dye. Panchromatic organic sensitizers are also being developed, for example the phenoxazine dye **TH304**[90] (Fig. 10) which contains a thiophene π-bridge that extends the absorption spectrum allowing for a broad IPCE from 300 to 920 nm with a maximum of 67% at 580 nm. Although the final efficiency is only 3%, the extension of its light harvesting capability to the near-IR is very promising.

An altogether different approach to achieve panchromatic absorption of DSSCs involves the co-sensitization of two or more dyes with complementary absorption spectra. Porphyrins, phthalocyanines, naphthalocyanines, cyanines and squarines all display intense absorption bands at lower energies making them excellent candidates for co-sensitization studies since they show an optical window over a large region of the visible spectrum allowing them to be combined with sensitizers that absorb in this part of the spectrum. Despite the many studies present in the literature and though co-sensitized DSSC devices generally show improved light-harvesting, they also usually show poorer overall efficiencies when compared to reference devices made from the individual sensitizers alone. One reason for this seems rather straightforward in that there is only a finite number of anchoring sites on the TiO₂ surface so any improvement in IPCE in one part of the spectrum by the introduction of a given sensitizer may be offset by poorer performance in IPCE in another part due to the removal of the other sensitizer dye(s). Another reason for poor performance of co-sensitized DSSCs is the deactivation of dye excited states due to energy or electron transfer processes between the different sensitizers.

In spite of this, there are some examples of successful combinations of dyes resulting in both increased light harvesting and improved cell efficiencies. In a study by Torres and co-workers[91] involving the phthalocyanine **TT1** and the organic dye **JK2**, co-sensitized devices yielded an overall cell efficiency of 7.74%, which was higher than the reference devices, with photoresponse extending up to 750 nm and with an IPCE of 72% at 690 nm corresponding to the Q-band of **TT1**. Wang and Zhang[92] combined three organic sensitizers absorbing in different regions of the UV-visible: a yellow merocyanine dye (λ_{max} at 380 nm), a red hemicyanine dye (λ_{max} at 535 nm) and a blue squarylium cyanine dye (λ_{max} at 642 nm). Co-sensitized devices showed a broad absorption from 350 to 750 nm giving an overall efficiency of 6.5%, which was higher than reference devices made with each individual sensitizer only. Co-sensitization of these three dyes resulted in reduced aggregation and improvements in injection efficiencies
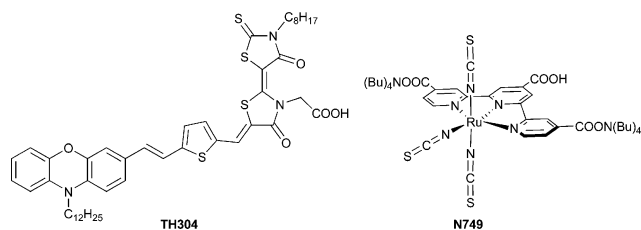

Fig. 10 Chemical structure of dyes **TH304** and **N749**.

and photocurrent. Ogura and co-workers[93] co-sensitized using the black dye **N749** and the indoline dye **D131** with devices achieving a power conversion efficiency of 11%, higher than the reference devices and indeed the highest for any co-sensitized DSSC. Keeping the different dye species isolated from one another by selectively positioning them on the TiO_2 electrode was the aim of two recent co-sensitization studies. Hayese and co-workers[94] co-sensitized nanocrystalline TiO_2 with black dye **N749** and the organic dye **NK3705**. Under pressurized CO_2 conditions and controlled time, **N749** uptake occurs faster than the normal dipping sensitization procedure, and so the dye occupies the upper microns of the TiO_2 film. Subsequent dipping with **NK3705** sensitizes the dye-free lower microns of the film next to the glass contact, producing a bilayer structure. The resulting device shows a broad IPCE curve from 300 to 900 nm, exceeding 70% from 400 to 650 nm, and an improved overall efficiency of 9.16% when compared to the reference devices. In another study Park and co-workers[95] applied a column chromatography method to achieve similar selective positioning of dyes on nanocrystalline TiO_2. The insertion of polystyrene into the pores of the TiO_2 retards the flow rate of the mobile phase (the dye solution for adsorption and an aqueous solution of NaOH and polypropyleneglycol for desorption) and thus, allows the selective positioning of three dyes (an organic dye **P5**, **N719** and **N749**) at different depths of the film. The resulting triple-dye-layer devices show a broad IPCE from 400 to 840 nm and improved overall efficiencies of 4.8% when compared to reference devices.

The problem of limited anchoring sites for sensitizers on the TiO_2 electrode is a significant one for co-sensitization studies. Several strategies have been used to overcome this. One method is based on the controlled sensitization of TiO_2 in which dye sensitized films are covered with a layer of Al_2O_3 and onto which a secondary monolayer of dye is deposited.[88,96] The layer of Al_2O_3 has duel functionality: it allows for increased dye adsorption onto the TiO_2 electrode and with the selection of suitable sensitizers with suitable re–dox properties it also facilitates the formation of a hole-transfer cascade in which holes are shuttled from the inner dye layer to the outer dye layer, increasing the distance between charge separated species and retarding charge recombination. The best results have been obtained using the sensitizer **JK2** and a squarine dye **SQ1** in the configuration TiO_2/**JK2**/Al_2O_3/**SQ1**[88] whose IPCE extends from 350 to 700 nm and reaches 85% at 453 nm (absorption band of **JK2**) and 79% at 660 nm (absorption band of **SQ1**) and an overall cell efficiency of 8.65% which is higher than the reference devices.

Another strategy which tries to solve the problem of limited space on the TiO_2 surface involves Förster resonance energy transfer (FRET) from a "relay" dye to a secondary "sensitizing" dye which utilizes this energy to inject electrons into the TiO_2 (Fig. 11). This requires the strong overlap of the emission spectrum of the relay dye with the absorption spectrum of the sensitizing dye for effective FRET. In this way panchromatic sensitization is possible with the relay dye absorbing photons at shorter wavelengths (the blue/green part of the spectrum) and transferring this energy to the sensitizer dye that absorbs in the red/near-IR region of the spectrum.
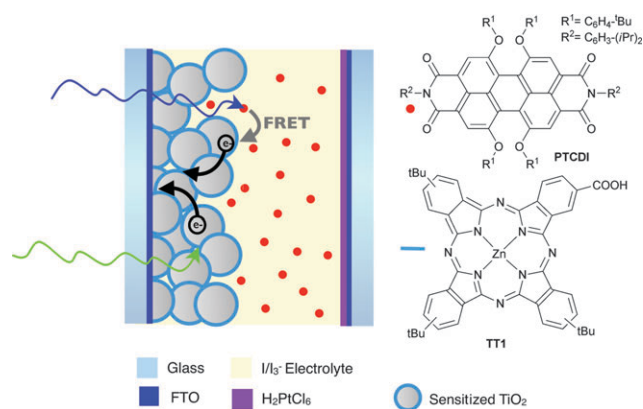

Fig. 11 Schematic view of the energy transfer relay based DSSC using the perylene **PTCDI** and phthalocyanine dye **TT1**.

Siegers and co-workers[97] used just such a strategy by employing a dyad sensitizer which consisted of the organic dye **Fluorol 7GA** acting as the relay dye which is covalently linked to the Ru(II) polypyridyl complex **[Ru(dcbpy)$_2$(acac)]Cl** that is itself attached to the TiO_2 surface. Devices made with this dyad sensitizer show enhanced IPCE spectra when compared to reference cells consisting of the polypyridyl complex only. However only a negligible increase in overall device efficiency was observed. More recently McGehee and coworkers[98] presented a novel design where the higher energy photons are absorbed by the perylene dye **PTCDI** which is dissolved in the cell electrolyte and undergoes FRET to the phthalocyanine **TT1** which is anchored to the TiO_2 surface (Fig. 11). The presence of the relay dye in the electrolyte allows for a full monolayer of **TT1** to anchor to the TiO_2 electrode. Devices made in this way show improved IPCE spectra when compared to reference devices with an increase in overall cell efficiency. The same concept has been applied in solid state solar cells with **N877** as the donor and **SQ1** as the acceptor.[99]

5. Supramolecular sensitizers

Supramolecular interactions involving sensitizer dyes immobilized onto nanocyrstalline TiO_2 electrodes can be exploited in DSSCs offering further exciting possibilities for optimization of these devices. Despite this however, there are surprisingly few examples in the literature. The few studies conducted can be divided into the following categories: (i) dye sensitizer encapsulation by macrocycles, (ii) host–guest ion binding dye sensitizers and (iii) self assembly of dye monolayers onto the TiO_2 surface *via* supramolecular interactions.

5.1 Rotaxane-encapsulated dye structures

Haque and co-workers[100] employed an azobenzene based dye which was threaded through an α-cyclodextrin ring (Fig. 12a). The formation of this rotaxane was carried out in solution and the entire structure was then immobilized onto nanocrystalline TiO_2 film through the cyclodextrin macrocycle. Transient absorption spectroscopy studies demonstrated that charge recombination is significantly retarded in TiO_2 films

α-CD n = 1
β-CD n = 2
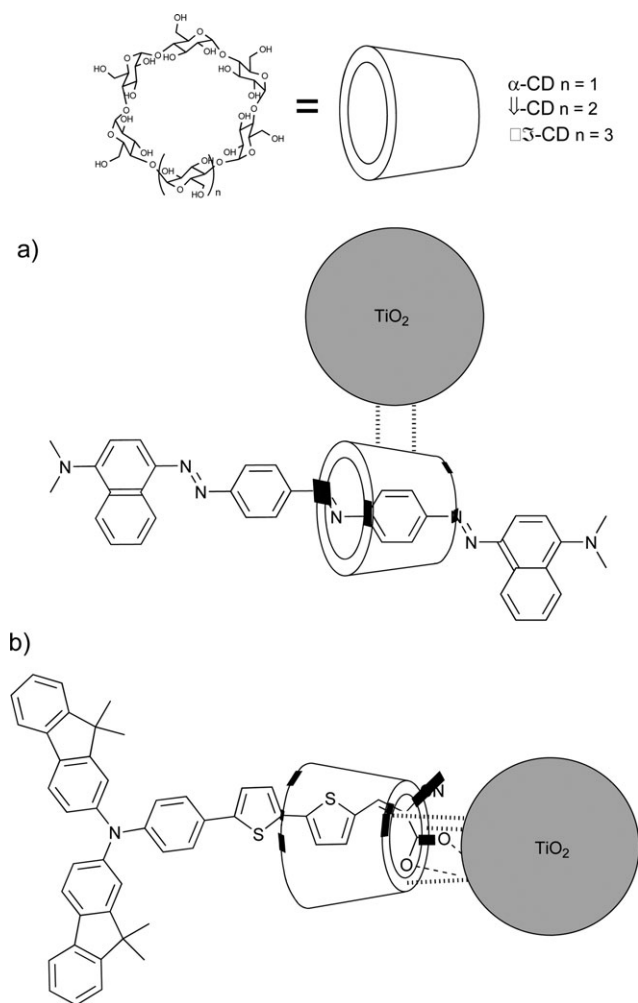γ-CD n = 3

a)

TiO₂

b)

Fig. 12 Rotaxane-encapsulated dye structures composed of a cyclodextrin ring and (a) an azobenzene based dye and (b) **JK2**.

sensitized with the encapsulated dye compared to films sensitized with non-encapsulated reference dye indicating that the cyclodextrin acts as an insulating shield between injected electrons in the TiO₂ and the oxidised dye. Ko and co-workers[101] also used this strategy to control interfacial electron transfer at the TiO₂ surface. However in this study nanocrytalline TiO₂ films were first pretreated with α-, β- and γ-cyclodextrin followed by complexation with the organic dye **JK2** on the film surface resulting in the formation of a rotaxane stoppered by the arylamino moiety at one extremity and by the TiO₂ particle at the other (Fig. 12b). DSSC devices made with β-cyclodextrin encapsulated **JK2** showed increased J_{sc}, V_{oc} and an improvement in overall efficiency (8.65%), when compared to reference devices made with **JK2** only (7.42%). The increased V_{oc} and efficiency were rationalised in terms of retardation of interfacial charge recombination processes and this was confirmed by photovoltage transient and electrochemical impedance measurements.

5.2 Host–guest ion binding dye sensitizers

It has been widely shown that the conduction band edge of nanocrystalline TiO₂ is extremely sensitive to the presence of
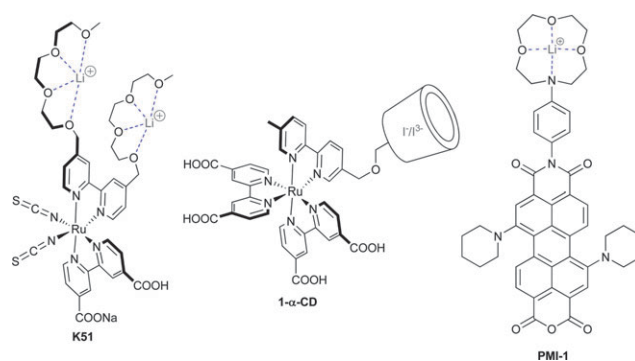

Fig. 13 Chemical structure of host–guest ion binding sensitizers **K51**, **1-α-CD** and **PMI-1**.

cations in the electrolyte. When these cations are adsorbed onto the electrode surface they shift the band edge positively and this will manifest itself in lower device V_{oc}. Planells and co-workers[102] aimed at circumventing this problem by designing the perylene dye **PMI-1** which incorporates a Li⁺ coordinating crown ether into its structure (Fig. 13). Because this crown ether is positioned on the opposite end of the sensitizer structure with respect to the anchoring unit, the Li⁺ ions are trapped well away from the TiO₂ surface. ¹H-NMR and mass spectrometry studies revealed that the crown ether in **PMI-1** did in fact complex Li⁺ ions resulting in increased V_{oc} for DSSC devices made with this sensitizer. In a related study involving solid-state DSSCs employing OMeTAD as the hole-transporting material, Snaith and co-workers[103] used the Ru(II) bipyridyl complex **K51** (Fig. 13) containing polyethylene glycol chains to coordinate Li⁺ ions. DSSC devices made with this sensitizer showed an impressive 125 mV increase in V_{oc} and an improved cell efficiency (3.8%) compared to reference devices (3.2%).

Falaras and Pikramenou[104] designed the supramolecular host **1-α-CD** consisiting of a Ru(II) tris-bipyridyl core with an appended α-cyclodextrin ring (Fig. 13). In this case the function of the cyclodextrin is to complex I⁻/I₃⁻ from the electrolyte within the macrocycle cavity thereby facilitating efficient regeneration of dye cations by the red–ox electrolyte. This dye was used in solid-state DSSCs employing a composite polymer electrolyte. Devices showed increased J_{sc}, V_{oc} and overall efficiency (1.64%) with respect to reference devices (1.17%). The ability of **1-α-CD** to complex the red–ox couple leading to improved regeneration was confirmed using solar cell devices containing low I⁻/I₃⁻ concentrations. Under these conditions devices containing **1-α-CD** still showed higher V_{oc} values in comparison to devices made with the reference sensitizer.

5.3 Dye self-assembly *via* supramolecular interactions

Biomimicry of energy and electron transfer processes found in nature such as those in photosynthetic reaction centres has received much attention.[105] There are many examples of self-assembled donor–acceptor supramolecular complexes in solution involving dyes such as porphyrins and phthalocyanines as the donor.[106,107] Supramolecular complexes have also been immobilized onto electrode surfaces.[108–110] For example, in a recent paper Imahori and co-workers[110] were able to assemble
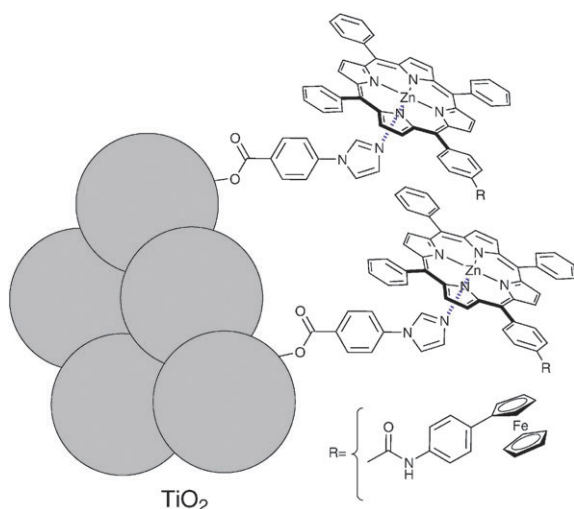
Fig. 14 Supramolecular axially ligated porphyrin DSSC.

stepwise supramolecular arrays of porphyrin and fullerenes onto a flat SnO$_2$ electrode. A maximum IPCE of 21% was recorded which compared favourably to other donor–acceptor arrays on electrodes.

Self-assembly of dyes onto nanocrystalline TiO$_2$ surfaces *via* supramolecular interactions is extremely attractive for DSSCs as it eases the structural requirements on sensitizers as the need for anchoring groups becomes redundant meaning far simpler synthetic routes and purification/separation steps. In a study by D'Souza and co-workers[111] a series of nitrogenous ligands covalently linked to a nanocrystalline TiO$_2$ film were used to coordinate to a series of zinc porphyrin sensitizers which do not contain any anchoring groups (Fig. 14). These ligands co-ordinate the metal centres of the porphyrin sensitizers resulting in dye sensitization of the TiO$_2$ electrodes. DSSC devices made from the porphyrin-ferrocene dyad complex (Fig. 14) showed modest IPCE of 37% at the Soret band of this sensitizer and an overall efficiency of 0.56%.

Conclusions

This review has been written with the aim of highlighting how targeting a single component of the DSSC, namely the dye sensitizer, can strongly determine overall device efficiency. That by subtly tweaking the molecular structure of the dye sensitizer electron injection can be improved or harmful electron transfer pathways such as recombination with the oxidized dye or red–ox electrolyte can be limited. Moreover, it is hoped that it has been demonstrated that dye sensitizer structure and consequently function in DSSCs are in continuous evolution, with the ultimate goal of optimizing device efficiency principally through the control of processes occurring at the molecular level.

The progress DSSC research has made up until now has been extremely encouraging. However, control of interfacial processes and maximizing light harvesting as well as resolving long-term stability issues will be challenging and will indeed take some time yet.

References

1 E. Galoppini, J. Rochford, H. H. Chen, G. Saraf, Y. C. Lu, A. Hagfeldt and G. Boschloo, *J. Phys. Chem. B*, 2006, **110**, 16159–16161.
2 Y. Bai, Y. M. Cao, J. Zhang, M. Wang, R. Z. Li, P. Wang, S. M. Zakeeruddin and M. Gratzel, *Nat. Mater.*, 2008, **7**, 626–630.
3 G. K. Mor, S. Kim, M. Paulose, O. K. Varghese, K. Shankar, J. Basham and C. A. Grimes, *Nano Lett.*, 2009, **9**, 4250–4257.
4 H. J. Snaith, A. J. Moule, C. Klein, K. Meerholz, R. H. Friend and M. Gratzel, *Nano Lett.*, 2007, **7**, 3372–3376.
5 N. A. Anderson and T. Lian, *Coord. Chem. Rev.*, 2004, **248**, 1231–1246.
6 S. Ardo and G. J. Meyer, *Chem. Soc. Rev.*, 2009, **38**, 115–164.
7 R. Katoh, A. Furube, A. V. Barzykin, H. Arakawa and M. Tachiya, *Coord. Chem. Rev.*, 2004, **248**, 1195–1213.
8 K. Schwarzburg, R. Ernstorfer, S. Felber and F. Willig, *Coord. Chem. Rev.*, 2004, **248**, 1259–1270.
9 D. F. Watson and G. J. Meyer, *Annu. Rev. Phys. Chem.*, 2005, **56**, 119–156.
10 R. A. Marcus and N. Sutin, *Biochim. Biophys. Acta Bioenergetics*, 1985, **811**, 265–322.
11 R. A. Marcus, *J. Chem. Phys.*, 1965, **43**, 679–701.
12 H. Gerischer, *Surf. Sci.*, 1969, **18**, 97–122.
13 G. Benko, M. Hilgendorff, A. P. Yartsev and V. Sundstrom, *J. Phys. Chem. B*, 2001, **105**, 967–974.
14 T. Hannappel, B. Burfeindt, W. Storck and F. Willig, *J. Phys. Chem. B*, 1997, **101**, 6799–6802.
15 K. Hara, Z. S. Wang, T. Sato, A. Furube, R. Katoh, H. Sugihara, Y. Dan-Oh, C. Kasada, A. Shinpo and S. Suga, *J. Phys. Chem. B*, 2005, **109**, 15476–15482.
16 R. Huber, J. E. Moser, M. Gratzel and J. Wachtveitl, *J. Phys. Chem. B*, 2002, **106**, 6494–6499.
17 T. Kitamura, M. Ikeda, K. Shigaki, T. Inoue, N. A. Anderson, X. Ai, T. Q. Lian and S. Yanagida, *Chem. Mater.*, 2004, **16**, 1806–1812.
18 Y. Tachibana, S. A. Haque, I. P. Mercer, J. R. Durrant and D. R. Klug, *J. Phys. Chem. B*, 2000, **104**, 1198–1205.
19 Y. Tachibana, J. E. Moser, M. Gratzel, D. R. Klug and J. R. Durrant, *J. Phys. Chem.*, 1996, **100**, 20056–20062.
20 C. Zimmermann, F. Willig, S. Ramakrishna, B. Burfeindt, B. Pettinger, R. Eichberger and W. Storck, *J. Phys. Chem. B*, 2001, **105**, 9245–9253.
21 S. Kim, J. K. Lee, S. O. Kang, J. Ko, J. H. Yum, S. Fantacci, F. De Angelis, D. Di Censo, M. K. Nazeeruddin and M. Gratzel, *J. Am. Chem. Soc.*, 2006, **128**, 16701–16707.
22 Q. Wang, W. M. Carnpbell, E. E. Bonfantani, K. W. Jolley, D. L. Officer, P. J. Walsh, K. Gordon, R. Humphry-Baker, M. K. Nazeeruddin and M. Gratzel, *J. Phys. Chem. B*, 2005, **109**, 15397–15409.
23 C. W. Lee, H. P. Lu, C. M. Lan, Y. L. Huang, Y. R. Liang, W. N. Yen, Y. C. Liu, Y. S. Lin, E. W. G. Diau and C. Y. Yeh, *Chem. Eur. J.*, 2009, **15**, 1403–1412.
24 A. Mishra, M. K. R. Fischer and P. Bauerle, *Angew. Chem., Int. Ed.*, 2009, **48**, 2474–2499.
25 J. J. Cid, M. Garcia-Iglesias, J. H. Yum, A. Forneli, J. Albero, E. Martinez-Ferrero, P. Vazquez, M. Gratzel, M. K. Nazeeruddin, E. Palomares and T. Torres, *Chem. Eur. J.*, 2009, **15**, 5130–5137.
26 J. B. Asbury, E. Hao, Y. Q. Wang, H. N. Ghosh and T. Q. Lian, *J. Phys. Chem. B*, 2001, **105**, 4545–4557.
27 J. B. Asbury, E. C. Hao, Y. Q. Wang and T. Q. Lian, *J. Phys. Chem. B*, 2000, **104**, 11957–11964.

28 R. Argazzi, C. A. Bignozzi, T. A. Heimer and G. J. Meyer, *Inorg. Chem.*, 1997, **36**, 2–3.

29 T. A. Heimer, S. T. Darcangelis, F. Farzad, J. M. Stipkala and G. J. Meyer, *Inorg. Chem.*, 1996, **35**, 5319–5324.

30 P. Piotrowiak, E. Galoppini, Q. Wei, G. J. Meyer and R. Wiewior, *J. Am. Chem. Soc.*, 2003, **125**, 5278–5279.

31 A. Morandeira, I. Lopez-Duarte, M. V. Martinez-Diaz, B. O'Regan, C. Shuttle, N. A. Haji-Zainulabidin, T. Torres, E. Palomares and J. R. Durrant, *J. Am. Chem. Soc.*, 2007, **129**, 9250–9251.

32 E. Palomares, M. V. Martinez-Diaz, S. A. Haque, T. Torres and J. R. Durrant, *Chem. Commun.*, 2004, 2112–2113.

33 Y. Tachibana, S. A. Haque, I. P. Mercer, J. E. Moser, D. R. Klug and J. R. Durrant, *J. Phys. Chem. B*, 2001, **105**, 7424–7431.

34 J. J. He, G. Benko, F. Korodi, T. Polivka, R. Lomoth, B. Akermark, L. C. Sun, A. Hagfeldt and V. Sundstrom, *J. Am. Chem. Soc.*, 2002, **124**, 4922–4932.

35 D. Liu, R. W. Fessenden, G. L. Hug and P. V. Kamat, *J. Phys. Chem. B*, 1997, **101**, 2583–2590.

36 S. Tatay, S. A. Haque, B. O'Regan, J. R. Durrant, W. J. H. Verhees, J. M. Kroon, A. Vidal-Ferran, P. Gavina and E. Palomares, *J. Mater. Chem.*, 2007, **17**, 3037–3044.

37 A. Kay and M. Gratzel, *J. Phys. Chem.*, 1993, **97**, 6272–6277.

38 K. Hara, Y. Dan-Oh, C. Kasada, Y. Ohga, A. Shinpo, S. Suga, K. Sayama and H. Arakawa, *Langmuir*, 2004, **20**, 4205–4210.

39 S. A. Haque, Y. Tachibana, R. L. Willis, J. E. Moser, M. Gratzel, D. R. Klug and J. R. Durrant, *J. Phys. Chem. B*, 2000, **104**, 538–547.

40 J. Nelson, *Phys. Rev. B: Condens. Matter Mater. Phys.*, 1999, **59**, 15374–15380.

41 J. Nelson and R. E. Chandler, *Coord. Chem. Rev.*, 2004, **248**, 1181–1194.

42 J. N. Clifford, G. Yahioglu, L. R. Milgrom and J. R. Durrant, *Chem. Commun.*, 2002, 1260–1261.

43 R. Argazzi, C. A. Bignozzi, T. A. Heimer, F. N. Castellano and G. J. Meyer, *J. Am. Chem. Soc.*, 1995, **117**, 11815–11816.

44 N. Hirata, J. J. Lagref, E. J. Palomares, J. R. Durrant, M. K. Nazeeruddin, M. Gratzel and D. Di Censo, *Chem. Eur. J.*, 2004, **10**, 595–602.

45 J. N. Clifford, E. Palomares, M. K. Nazeeruddin, M. Gratzel, J. Nelson, X. Li, N. J. Long and J. R. Durrant, *J. Am. Chem. Soc.*, 2004, **126**, 5225–5233.

46 H. J. Snaith, *Adv. Funct. Mater.*, 2010, **20**, 13–19.

47 S. Ito, P. Liska, P. Comte, R. L. Charvet, P. Pechy, U. Bach, L. Schmidt-Mende, S. M. Zakeeruddin, A. Kay, M. K. Nazeeruddin and M. Gratzel, *Chem. Commun.*, 2005, 4351–4353.

48 J. E. Kroeze, N. Hirata, S. Koops, M. K. Nazeeruddin, L. Schmidt-Mende, M. Gratzel and J. R. Durrant, *J. Am. Chem. Soc.*, 2006, **128**, 16376–16383.

49 P. Wang, S. M. Zakeeruddin, P. Comte, R. Charvet, R. Humphry-Baker and M. Gratzel, *J. Phys. Chem. B*, 2003, **107**, 14336–14341.

50 S. M. Zakeeruddin, M. K. Nazeeruddin, R. Humphry-Baker, P. Pechy, P. Quagliotto, C. Barolo, G. Viscardi and M. Gratzel, *Langmuir*, 2002, **18**, 952–954.

51 Y. J. Liu, N. Xiang, X. M. Feng, P. Shen, W. P. Zhou, C. Weng, B. Zhao and S. T. Tan, *Chem. Commun.*, 2009, 2499–2501.

52 A. Forneli, M. Planells, M. A. Sarmentero, E. Martinez-Ferrero, B. C. O'Regan, P. Ballester and E. Palomares, *J. Mater. Chem.*, 2008, **18**, 1652–1658.

53 N. Koumura, Z. S. Wang, S. Mori, M. Miyashita, E. Suzuki and K. Hara, *J. Am. Chem. Soc.*, 2006, **128**, 14256–14257.

54 H. Choi, C. Baik, S. O. Kang, J. Ko, M. S. Kang, M. K. Nazeeruddin and M. Gratzel, *Angew. Chem., Int. Ed.*, 2008, **47**, 327–330.

55 Z. S. Wang, N. Koumura, Y. Cui, M. Takahashi, H. Sekiguchi, A. Mori, T. Kubo, A. Furube and K. Hara, *Chem. Mater.*, 2008, **20**, 3993–4003.

56 S. Ito, H. Miura, S. Uchida, M. Takata, K. Sumioka, P. Liska, P. Comte, P. Pechy and M. Graetzel, *Chem. Commun.*, 2008, 5194–5196.

57 J. Bisquert, A. Zaban, M. Greenshtein and I. Mora-Sero, *J. Am. Chem. Soc.*, 2004, **126**, 13550–13559.

58 A. J. Mozer, P. Wagner, D. L. Officer, G. G. Wallace, W. M. Campbell, M. Miyashita, K. Sunahara and S. Mori, *Chem. Commun.*, 2008, 4741–4743.

59 B. C. O'Regan, I. Lopez-Duarte, M. V. Martinez-Diaz, A. Forneli, J. Albero, A. Morandeira, E. Palomares, T. Torres and J. R. Durrant, *J. Am. Chem. Soc.*, 2008, **130**, 2906–2907.

60 M. Miyashita, K. Sunahara, T. Nishikawa, Y. Uemura, N. Koumura, K. Hara, A. Mori, T. Abe, E. Suzuki and S. Mori, *J. Am. Chem. Soc.*, 2008, **130**, 17874–17881.

61 B. C. O'Regan, K. Walley, M. Juozapavicius, A. Anderson, F. Matar, T. Ghaddar, S. M. Zakeeruddin, C. Klein and J. R. Durrant, *J. Am. Chem. Soc.*, 2009, **131**, 3541–3548.

62 A. Reynal, A. Forneli, E. Martinez-Ferrero, A. Sanchez-Diaz, A. Vidal-Ferran, B. C. O'Regan and E. Palomares, *J. Am. Chem. Soc.*, 2008, **130**, 13558–13567.

63 B. O'Regan and M. Gratzel, *Nature*, 1991, **353**, 737–740.

64 N. Robertson, *Angew. Chem., Int. Ed.*, 2006, **45**, 2338–2345.

65 M. K. Nazeeruddin, A. Kay, I. Rodicio, R. Humphrybaker, E. Muller, P. Liska, N. Vlachopoulos and M. Gratzel, *J. Am. Chem. Soc.*, 1993, **115**, 6382–6390.

66 M. K. Nazeeruddin, S. M. Zakeeruddin, R. Humphry-Baker, M. Jirousek, P. Liska, N. Vlachopoulos, V. Shklover, C. H. Fischer and M. Gratzel, *Inorg. Chem.*, 1999, **38**, 6298–6305.

67 M. K. Nazeeruddin, P. Pechy and M. Gratzel, *Chem. Commun.*, 1997, 1705–1706.

68 M. K. Nazeeruddin, P. Pechy, T. Renouard, S. M. Zakeeruddin, R. Humphry-Baker, P. Comte, P. Liska, L. Cevey, E. Costa, V. Shklover, L. Spiccia, G. B. Deacon, C. A. Bignozzi and M. Gratzel, *J. Am. Chem. Soc.*, 2001, **123**, 1613–1624.

69 P. Wang, C. Klein, R. Humphry-Baker, S. M. Zakeeruddin and M. Gratzel, *J. Am. Chem. Soc.*, 2005, **127**, 808–809.

70 D. B. Kuang, C. Klein, S. Ito, J. E. Moser, R. Humphry-Baker, N. Evans, F. Duriaux, C. Graetzel, S. M. Zakeeruddin and M. Graetzel, *Adv. Mater.*, 2007, **19**, 1133–1137.

71 F. Gao, Y. Wang, D. Shi, J. Zhang, M. K. Wang, X. Y. Jing, R. Humphry-Baker, P. Wang, S. M. Zakeeruddin and M. Gratzel, *J. Am. Chem. Soc.*, 2008, **130**, 10720–10728.

72 C. Y. Chen, S. J. Wu, C. G. Wu, J. G. Chen and K. C. Ho, *Angew. Chem., Int. Ed.*, 2006, **45**, 5822–5825.

73 C. Y. Chen, M. K. Wang, J. Y. Li, N. Pootrakulchote, L. Alibabaei, C. H. Ngoc-le, J. D. Decoppet, J. H. Tsai, C. Gratzel, C. G. Wu, S. M. Zakeeruddin and M. Gratzel, *ACS Nano*, 2009, **3**, 3103–3109.

74 K. Hara, T. Sato, R. Katoh, A. Furube, T. Yoshihara, M. Murai, M. Kurashige, S. Ito, A. Shinpo, S. Suga and H. Arakawa, *Adv. Funct. Mater.*, 2005, **15**, 246–252.

75 K. Hara, K. Sayama, Y. Ohga, A. Shinpo, S. Suga and H. Arakawa, *Chem. Commun.*, 2001, 569–570.

76 K. Hara, T. Sato, R. Katoh, A. Furube, Y. Ohga, A. Shinpo, S. Suga, K. Sayama, H. Sugihara and H. Arakawa, *J. Phys. Chem. B*, 2003, **107**, 597–606.

77 K. Hara, M. Kurashige, Y. Dan-oh, C. Kasada, A. Shinpo, S. Suga, K. Sayama and H. Arakawa, *New J. Chem.*, 2003, **27**, 783–785.

78 T. Horiuchi, H. Miura and S. Uchida, *Chem. Commun.*, 2003, 3036–3037.

79 T. Horiuchi, H. Miura, K. Sumioka and S. Uchida, *J. Am. Chem. Soc.*, 2004, **126**, 12218–12219.

80 S. Ito, S. M. Zakeeruddin, R. Humphry-Baker, P. Liska, R. Charvet, P. Comte, M. K. Nazeeruddin, P. Pechy, M. Takata, H. Miura, S. Uchida and M. Gratzel, *Adv. Mater.*, 2006, **18**, 1202–1205.

81 G. L. Zhang, H. Bala, Y. M. Cheng, D. Shi, X. J. Lv, Q. J. Yu and P. Wang, *Chem. Commun.*, 2009, 2198–2200.

82 S. Hwang, J. H. Lee, C. Park, H. Lee, C. Kim, M. H. Lee, W. Lee, J. Park, K. Kim and N. G. Park, *Chem. Commun.*, 2007, 4887–4889.

83 D. P. Hagberg, J. H. Yum, H. Lee, F. De Angelis, T. Marinado, K. M. Karlsson, R. Humphry-Baker, L. C. Sun, A. Hagfeldt, M. Gratzel and M. K. Nazeeruddin, *J. Am. Chem. Soc.*, 2008, **130**, 6259–6266.

84 H. Qin, S. Wenger, M. Xu, F. Gao, X. Jing, P. Wang, S. M. Zakeeruddin and M. Gratzel, *J. Am. Chem. Soc.*, 2008, **130**, 9202–9203.

85 W. D. Zeng, Y. M. Cao, Y. Bai, Y. H. Wang, Y. S. Shi, M. Zhang, F. F. Wang, C. Y. Pan and P. Wang, *Chem. Mater.*, 2010, **22**, 1915–1925.

86 H. Imahori, T. Umeyama and S. Ito, *Acc. Chem. Res.*, 2009, **42**, 1809–1818.

87 W. M. Campbell, K. W. Jolley, P. Wagner, K. Wagner, P. J. Walsh, K. C. Gordon, L. Schmidt-Mende,

M. K. Nazeeruddin, Q. Wang, M. Gratzel and D. L. Officer, *J. Phys. Chem. C*, 2007, **111**, 11760–11762.

88 H. Choi, S. Kim, S. O. Kang, J. J. Ko, M. S. Kang, J. N. Clifford, A. Forneli, E. Palomares, M. K. Nazeeruddin and M. Gratzel, *Angew. Chem., Int. Ed.*, 2008, **47**, 8259–8263.

89 N. Onozawa-Komatsuzaki, M. Yanagida, T. Funaki, K. Kasuga, K. Sayama and H. Sugihara, *Inorg. Chem. Commun.*, 2009, **12**, 1212–1215.

90 H. N. Tian, X. C. Yang, R. K. Chen, A. Hagfeldt and L. C. Sun, *Energy Environ. Sci.*, 2009, **2**, 674–677.

91 J. J. Cid, J. H. Yum, S. R. Jang, M. K. Nazeeruddin, E. Martinez-Ferrero, E. Palomares, J. Ko, M. Gratzel and T. Torres, *Angew. Chem., Int. Ed.*, 2007, **46**, 8358–8362.

92 Y. S. Chen, Z. H. Zeng, C. Li, W. B. Wang, X. S. Wang and B. W. Zhang, *New J. Chem.*, 2005, **29**, 773–776.

93 R. Y. Ogura, S. Nakane, M. Morooka, M. Orihashi, Y. Suzuki and K. Noda, *Appl. Phys. Lett.*, 2009, **94**, 073308.

94 F. Inakazu, Y. Noma, Y. Ogomi and S. Hayase, *Appl. Phys. Lett.*, 2008, **93**, 093304.

95 K. Lee, S. W. Park, M. J. Ko, K. Kim and N. G. Park, *Nat. Mater.*, 2009, **8**, 665–671.

96 J. N. Clifford, E. Palomares, K. Nazeeruddin, R. Thampi, M. Gratzel and J. R. Durrant, *J. Am. Chem. Soc.*, 2004, **126**, 5670–5671.

97 C. Siegers, J. Hohl-Ebinger, B. Zimmerrnann, U. Wurfel, R. Mulhaupt, A. Hinsch and R. Haag, *ChemPhysChem*, 2007, **8**, 1548–1556.

98 B. E. Hardin, E. T. Hoke, P. B. Armstrong, J. H. Yum, P. Comte, T. Torres, J. M. J. Frechet, M. K. Nazeeruddin, M. Gratzel and M. D. McGehee, *Nat. Photonics*, 2009, **3**, 406–411.

99 J. H. Yum, B. E. Hardin, S. J. Moon, E. Baranoff, F. Nuesch, M. D. McGehee, M. Gratzel and M. K. Nazeeruddin, *Angew. Chem., Int. Ed.*, 2009, **48**, 9277–9280.

100 S. A. Haque, J. S. Park, M. Srinivasarao and J. R. Durrant, *Adv. Mater.*, 2004, **16**, 1177–1181.

101 H. Choi, S. O. Kang, J. Ko, G. Gao, H. S. Kang, M. S. Kang, M. K. Nazeeruddin and M. Gratzel, *Angew. Chem., Int. Ed.*, 2009, **48**, 5938–5941.

102 M. Planells, F. J. Cespedes-Guirao, L. Goncalves, A. Sastre-Santos, F. Fernandez-Lazaro and E. Palomares, *J. Mater. Chem.*, 2009, **19**, 5818–5825.

103 H. J. Snaith, S. M. Zakeeruddin, L. Schmidt-Mende, C. Klein and M. Gratzel, *Angew. Chem., Int. Ed.*, 2005, **44**, 6413–6417.

104 J. Faiz, A. I. Philippopoulos, A. G. Kontos, P. Falaras and Z. Pikramenou, *Adv. Funct. Mater.*, 2007, **17**, 54–58.

105 J.-M. Lehn, *Supramolecular Chemistry: Concepts and Perspectives*, VCH, Weinheim, Germany, 1995.

106 R. Chitta and F. D'Souza, *J. Mater. Chem.*, 2008, **18**, 1440–1471.

107 F. D'Souza and O. Ito, *Coord. Chem. Rev.*, 2005, **249**, 1410–1422.

108 T. Hasobe, H. Imahori, S. Fukuzumi and P. V. Kamat, *J. Phys. Chem. B*, 2003, **107**, 12105–12112.

109 H. Imahori and S. Fukuzumi, *Adv. Funct. Mater.*, 2004, **14**, 525–536.

110 A. Kira, T. Umeyama, Y. Matano, K. Yoshida, S. Isoda, J. K. Park, D. Kim and H. Imahori, *J. Am. Chem. Soc.*, 2009, **131**, 3198–3200.

111 N. K. Subbaiyan, C. A. Wijesinghe and F. D'Souza, *J. Am. Chem Soc.*, 2009, **131**, 14646–14647.